11th International Conference on Vibration Problems
Z. Dimitrovová *et al.* (eds.)
Lisbon, Portugal, 9-12 September 2013

SIMULATION AND EXPERIMENTAL VALIDATION OF THE DYNAMICS OF A DUAL-ROTOR VIBROACTUATOR

Ákos Miklós*[1], Zsolt Szabó[2]

[1]HAS-BUTE, Research Group on Dynamics of Machines and Vehicles, Nádor u. 7. 1051 Budapest, Hungary
miklosa@mm.bme.hu

[2]BUTE, Department of Applied Mechanics, Műegyetem rkp. 5. 1111 Budapest, Hungary
szazs@mm.bme.hu

Keywords: dual rotor vibroactuator, vibrotactor, mechanical synchronization.

Abstract. *In this work a novel design for small vibrotactors is presented, which makes it possible to produce vibrations with independently adjustable frequency and amplitude. This feature has been realized using two coaxially aligned eccentric rotors, which are driven by DC motors independently. The prototype of the device has been built, where mechanical components are integrated on a frame with two optical sensors for the measurement of angular velocity and phase shift. The system is equipped with a digital controller and other necessary electronic components. Simulations confirm the results of analytical investigations, and they allow us to model the sampling method of the signals of the angular velocity and phase shift between the rotors, furthermore to model the discrete behaviour of the digital controller, which is a PI controller for the angular velocities, and a PID controller for the phase shift. Finally, simulation results are compared to experimental ones, and advantages and limitations of the 4 DoF analytical model are also discussed.*

1 INTRODUCTION

The dual-rotor vibroactuator, which is presented in this work, is a novel concept for generating vibrations with increased performance, compared to common vibroactuators. Transmitting information by mechanical vibrations has become an essential way in many handheld devices [1]. Today's standard vibrotactors are eccentric rotors mounted on the shaft of a DC motor. This allows a very simple design, but as the frequency and the amplitude of the excited vibrations are not independent, the performance of such devices is limited. In most common applications for vibroactuators, like cell phones or video game controllers, the excited vibration has to be adjusted to the sensitivity of the user's skin, so frequencies much higher, than the optimum cannot be used, because of the too high amplitudes, and at frequencies, lower than the optimum the amplitude goes below the sensation threshold of the skin [2]. Also in experimental applications, where exact vibration parameters have to be set on-line, simple rotational vibroactuators cannot be used.

The dual-rotor vibroactuator concept, which is also called as Dual Excenter, solves the problem of the coupled vibration frequency and amplitude. In this concept two coaxially positioned eccentric rotors are used for generating vibrations, so at a given angular speed of the rotors the resulting eccentricity of the whole system can be adjusted by tuning the position of the rotors related to each other. This related position can be written as an angle between the rotors, later on *phase angle*, which is related to the amplitude of the excited vibration. Furthermore, the angular speed of the two rotors is related to the frequency of the excited vibration. So with the phase angle, the amplitude can be tuned between zero and a maximum value, defined by the mechanical design of the device and the current frequency, thus a wide range of sensation can be generated on the human skin, or the excitation for an experiment can be set properly. The method is showed on Figure 1, where different configurations are depicted. The smaller black circles show the centres of mass (CoM) of the rotors and the larger shows the common CoM of the two rotors, respectively. If the angular speeds of both rotors are the same, the common CoM moves on a circular path as well. Zero amplitude is only possible, if the eccentricities (mass×length) of both rotors are the same.
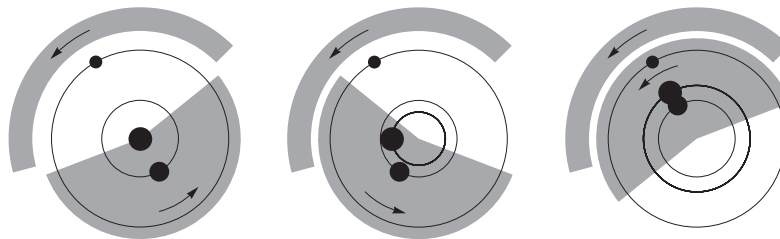

Figure 1: Different configurations of the rotors for zero, medium and maximum amplitude.

The Dual Excenter concept solves not only the problem of the constraint between frequency and amplitude, but it also enables some interesting working methods, showed in Figure 2. If the two rotors are turning in the same direction, but with different angular velocities, the resulting vibration will be a pulsating one. In case of opposite turning directions and with equal angular velocities, the vibration is one-directional rather than rotating, and with different angular speeds this direction also changes slowly.

Furthermore the concept also enables fast changes in vibration amplitudes without slowing down and speeding up again the rotation of the rotors, because only a change in the phase angle is necessary, which can be carried out faster, and more energy-efficient.
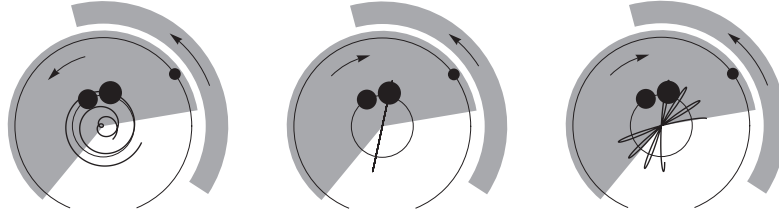
Figure 2: Further possible working modes of the Dual Excenter: pulsating, one-directional and direction changing vibration.

2   MECHANICAL MODEL OF THE DUAL-ROTOR VIBROACTUATOR

To investigate the feasibility of the novel Dual Excenter concept, a mechanical model has to be constructed. Doing this, the main components of such device have to be considered, which have significant influence on the dynamics of the system. One of the possible designs of the device is depicted on Figure 3.
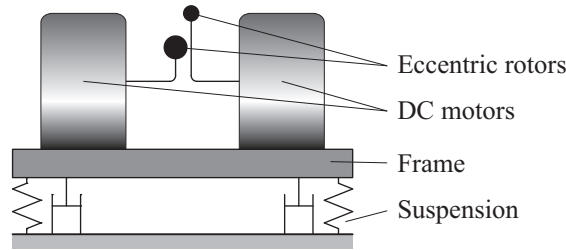

Figure 3: Main components of the Dual Excenter

The main parts of the device are the two eccentric rotors, the driving DC motors, which are mounted on the common frame. This frame is suspended on any object (like the human skin or the frame of a cell phone). In simple case the suspension can be considered as a system of springs and dampers.

Generally, the motion of the frame could be 6 degrees-of-freedom spatial motion, however for analytical investigations some simplifications could be introduced. If the suspension of the system is considered as isotropic, and the two CoMs of the eccentric rotors are rotating in the same plane (or approximately the same plane), the motion of the frame can be considered as planar motion. The plane of the motion is then normal to the common rotational axis [3]. The planar mechanical model of the device can be seen on Figure 4. Later, experiments show, that these simplifications do not limit the validity of the proposed mechanical model.

On Figure 4 point O is the origin of the global reference frame, which in case of undeformed springs coincides with the point C, which represents the common rotational axis of the rotors. The position of point C is given by the polar coordinates a and ϑ. Furthermore, the angular positions of the two rotors are given by the angle between the horizontal and the common bisector of the rotors, φ (which in turn indicates the angular position of the common CoM), and the angle between one rotor and the common bisector, δ, which actually is the half of the phase angle between the two rotors. So the mechanical model has 4 degrees-of-freedom. The suspension of the frame is parameterized by the spring stiffness k and damping coefficient c. m is the mass of the common frame, and m_0 and e are the mass and eccentricity (length) of both rotors, respectively. Also the mass moments of inertia of the rotors can be considered by parameter Θ for both rotors. The driving motors are considered by the torques T_1 and T_2, where stationary performance of the DC motors has been taken into account.
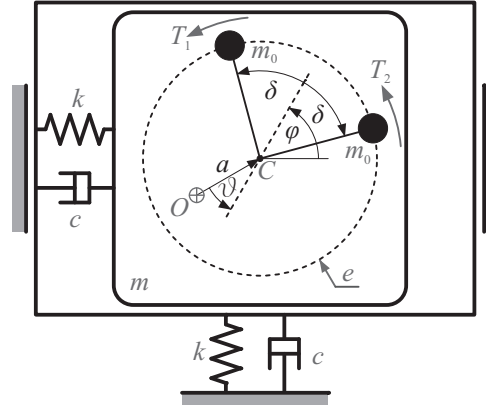
Figure 4: Planar mechanical model of the Dual Excenter

The derivation of the dimensionless equations of motion can be found in [3]. After investigating the steady state motions of the system, the formulae for a, ϑ and the sum and the difference between the driving voltages of the motors could be given as functions of the angular speed of the common CoM and the phase angle.

$$\Sigma U = \frac{2\zeta\lambda^5 \cos^2\Delta_0}{\left(1-\lambda^2\right)^2 + \left(2\zeta\lambda\right)^2} + r\lambda, \tag{1}$$

$$\Delta U = \frac{\lambda^4\left(1-\lambda^2\right)\cos\Delta_0 \sin\Delta_0}{\left(1-\lambda^2\right)^2 + \left(2\zeta\lambda\right)^2}, \tag{2}$$

where λ is the frequency ratio between the angular velocity $\dot{\varphi}$ and the natural frequency of the suspended frame. Δ_0 is the steady value of δ, ζ is the damping ratio of the suspended frame, r contains electric parameters of the driving motors and ΣU and ΔU are the dimensionless sum and the difference between the driving voltages, respectively.

That means also, that for every λ (which in turn corresponds to the first derivative of φ) and Δ_0, the driving voltages can be given, where the system can reach steady state motion, so even if the driving voltages are not equal, the rotors can have the same angular speeds. This phenomenon is caused by the mechanical synchronization between the two eccentric rotors. Mechanical synchronization was first investigated by Huygens, who experienced the synchronization of pendulum clocks attached to a common base [4]. Later many scientists worked on the theory of this phenomenon. Recently Leonov showed a general method to handle with phase synchronization in [5], and his current work on the in-phase synchronization of two metronome pendula shows, that there are still open problems in this area [6]. The work of Czolczynski *et al.* points out, that the mechanical synchronization occurs not only in unidirectional rotation of the eccentric rotors, but also with rotors turning in opposite direction [7].
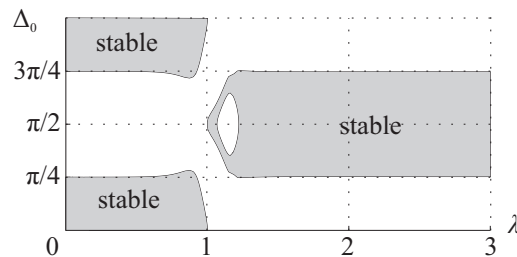

Figure 5: Characteristic linear stability chart for the Dual Excenter (with parameters listed in Table 1)

If the linear stability of every working point (λ, Δ_0) is investigated, one can see, that the synchronized motion is stable around $\Delta_0 = 0$ below the resonance frequency of the suspended frame, which is in-phase motion of the rotors, and around $\Delta_0 = \pi/2$ above the resonance frequency, which is anti-phase motion (see Figure 5).

In the following sections the mechanical synchronization of the system is investigated by simulations and experiments, and the stabilization of the whole working area of the Dual Excenter by a simple controller is analyzed.

3   SIMULATION RESULTS

For simulation purposes the chosen generalized coordinates, showed on Figure 4, are not convenient, because of the singularity of the polar coordinates around point O. For this reason instead of the polar coordinates of point C, translational coordinates x and y are introduced in simulations.
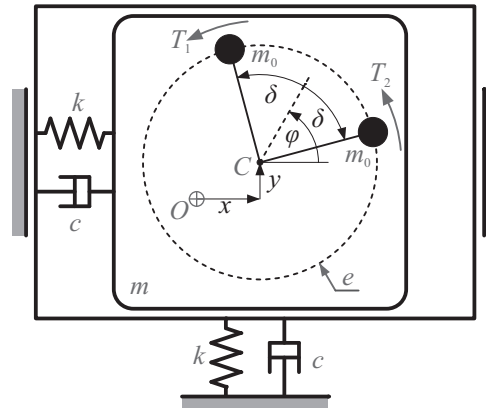

Figure 6: Mechanical model of the Dual Excenter with translational coordinates

The modified equations of motion can be derived with the Lagrangian equation of the second kind:

$$
\begin{bmatrix}
m + 2m_0 & 0 & -2e\,m_0 \cos\delta \sin\varphi & -2e\,m_0 \sin\delta \cos\varphi \\
0 & m + 2m_0 & 2e\,m_0 \cos\delta \cos\varphi & -2e\,m_0 \sin\delta \sin\varphi \\
-2e\,m_0 \cos\delta \sin\varphi & 2e\,m_0 \cos\delta \cos\varphi & 2e^2 m_0 + 2\Theta & 0 \\
-2e\,m_0 \sin\delta \cos\varphi & -2e\,m_0 \sin\delta \sin\varphi & 0 & 2e^2 m_0 + 2\Theta
\end{bmatrix}
\begin{bmatrix}
\ddot{x} \\ \ddot{y} \\ \ddot{\varphi} \\ \ddot{\delta}
\end{bmatrix} =
$$

$$
\begin{bmatrix}
-kx - c\dot{x} + 2e\,m_0 \left(\dot{\delta}^2 \cos\delta \cos\varphi - 2\dot{\delta}\dot{\varphi} \sin\delta \sin\varphi + \dot{\varphi}^2 \cos\delta \cos\varphi \right) \\
-ky - c\dot{y} + 2e\,m_0 \left(\dot{\delta}^2 \cos\delta \sin\varphi + 2\dot{\delta}\dot{\varphi} \sin\delta \cos\varphi + \dot{\varphi}^2 \cos\delta \sin\varphi \right) \\
k_t / R \left(u_1 + u_2 - 2k_e \dot{\varphi} \right) \\
k_t / R \left(u_1 - u_2 - 2k_e \dot{\delta} \right)
\end{bmatrix} . \tag{3}
$$

Based on the modified equations of motion numerical simulations have been carried out with the system parameters listed in Table 1, which are obtained from the experimental prototype device on Figure 7. The inputs for the simulation are the driving voltages of the two DC motors.
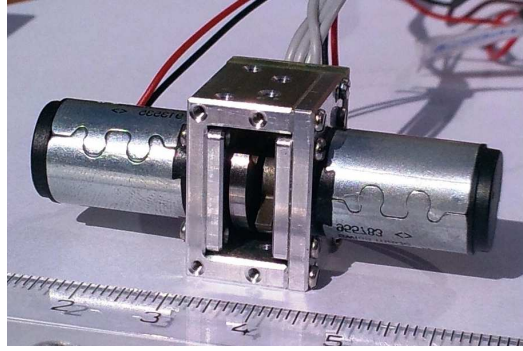
Figure 7: Prototype of the Dual Excenter

Name	Sign	Value	Unit
mass of the frame	m	42.1	g
eccentric mass of one rotor	m_0	1.6	g
inertia of one rotor	Θ	59.8	g·mm^2
eccentricity	e	2.1	mm
spring stiffness	k	5000	N/m
damping coefficient	c	30	N·s/m
torque constant of one motor	k_t	5.08	N·mm/A
speed constant of one motor	k_e	5.08	V·s/rad
electric resistance of one motor	R	11.3	Ω

Table 1: Parameters of the Dual Excenter prototype and simulation

First, the mechanical synchronization is investigated with different driving voltages, focusing on cases, where first the sum of the voltages changes, while the difference between them is held zero. The results of this simulation can be seen on Figure 8. The initial phase angle between the two rotors is about 2 radians. Then, as the frequency increases, the mechanical synchronization brings the rotors in-phase. After reaching the resonance of the suspended frame, the phase angle quickly changes from zero to π.
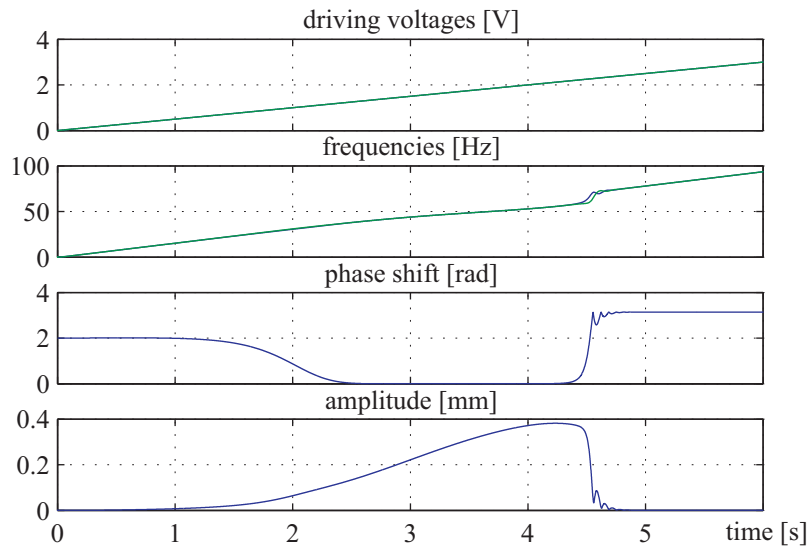

Figure 8: Stability of the system below and above the resonance frequency of the suspended frame

There is one more interesting effect: as the frequency approaches to the resonance, the amplitude of the vibration gets higher, which causes increased power consumption on the DC motors. This is called the jamming of the motors. So the over-passing on the resonance can only happen, if the driving voltage reaches a value large enough to cover this demand. This happens then with a characteristic jump in the frequency diagram.

In the second simulation the sum of the driving voltages is constant, and the difference between them is changed in steps. On Figure 9 the diagram on the left side shows the behaviour of the system below the resonance frequency, and on the right side above the resonance. One can see that the frequencies of both rotors are the same as long as the voltage difference reaches a maximal value. Then the mechanical synchronization disappears, and the rotors are turning with different angular velocities. As it could have been suspected, below the resonance with increasing voltage difference the system can be deviated from the in-phase (large amplitude) state, and the anti-phase domain is unstable. Above the resonance the behaviour is the opposite.
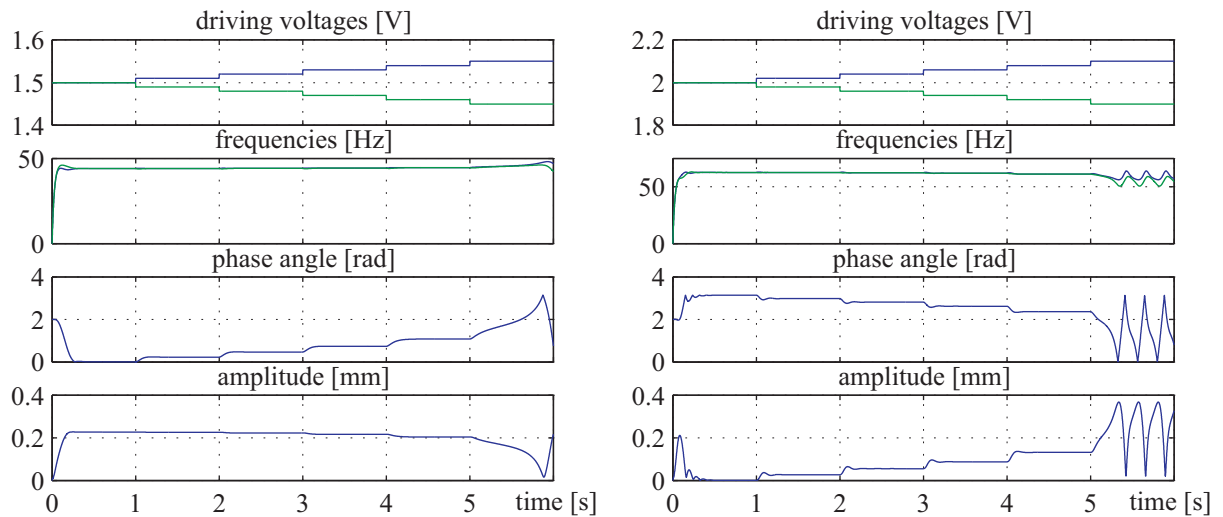

Figure 9: Influence of the voltage difference on phase shift below and above the resonance frequency

These results indicate that the system is capable to generate vibrations with different amplitudes at a given frequency, but the amplitude is limited to the stable region, and it depends on the resonance frequency of the suspended frame as well. This makes the robust and optimal application of the device not possible.

For this reason a simple control is applied onto the system. Control of such system has been done by Liu *et al.*, however the aim of their work was to achieve stable in-phase synchronization [8]. In this study only the feasibility of the control of the system is investigated, optimization of the control will be the subject of later research.

The analytical investigations as well the simulations showed that the frequency of the generated vibration depends mainly on the sum of the driving voltages, and the phase angle at a given frequency can be adjusted by the voltage difference. These two clearly define the driving voltages for the motors. The feedback for the control is the frequency and the phase angle, which can be measured e.g. by optical sensors on both rotors. In the current prototype the rotors are manufactured that way that the signal of the optical sensors changes in every turn twice. The frequencies f_1, f_2 and phase angle ε can be calculated from the time required for every signal change and from the delay between the changes of the two sensors, respectively. Knowing these values the input voltages can be given by Eqs. (4) and (5).

7

$$\Sigma u_{\text{ctrl}} = \Sigma u_{\text{steady}} + P_{\text{frq}} \left(f_{\text{desired}} - \frac{f_1 + f_2}{2} \right),$$ (4)

$$\Delta u_{\text{ctrl}} = \Delta u_{\text{steady}} + P_{\text{eps}} \left(\varepsilon_{\text{desired}} - \varepsilon \right) + D_{\text{eps}} \dot{\varepsilon} ,$$ (5)

where the steady voltage values can be calculated as approximation of Eqs. (1) and (2). The approximation is necessary because the exact value of the stiffness and damping of the suspension cannot be considered as known. The *P* and *D* parameters are proportional and differential gains, respectively. The first derivative of the phase angle can be obtained from the difference between the angular velocities.

With this control strategy simulations were carried out, where the effects of a digital control were taken into account, like digital sampling, time delay of the sampling of frequency and phase angle, time delay of control signal, and discrete values of the control signals. The results of a simulation can be seen on Figure 10. One can see that with control parameters optimized for a frequency around 80 Hz the control of the phase angle is possible with good performance. However, if the frequency decreases, the stability of the control loses because of increased time delays, and at higher frequencies the accuracy of the control deteriorates because of high forces, returning the system in stable regions.
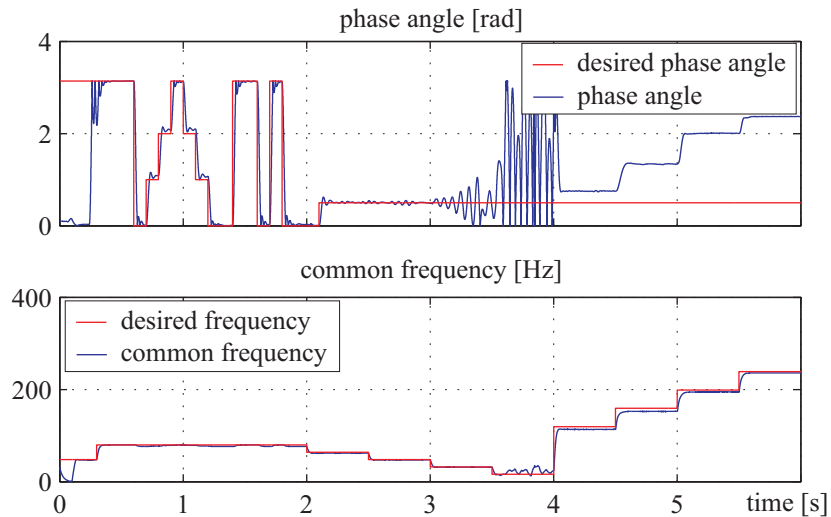

Figure 10: Performance of the controlled system for different angular velocity domains

4 EXPERIMENTAL RESULTS

The results obtained from simulation were validated by measurements on the prototype device showed on Figure 7. First the measurement according to simulation on the right side of Figure 9 was carried out, as it can be seen on Figure 11. Since the suspension parameters of the measurement were practically unknown (the device has been held by hand), the measurement and the simulation show very good match, so the possibility of the uncontrolled application has been verified, however the performance of such a device would be very poor since the stable phase angle range is limited.
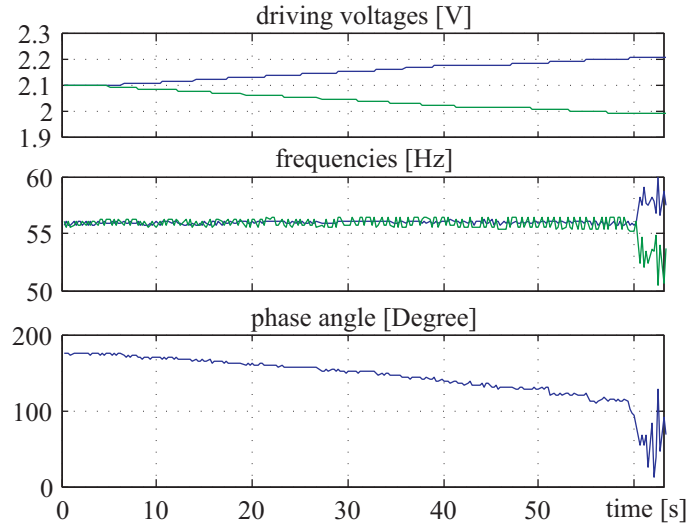
Figure 11: Measurement of the phase angle at different voltage differences above resonance

As it can be clearly seen, control is needed for the optimal and robust application of the device. For the prototype device a very similar control has been implemented as in Eqs. (4) and (5), with the difference, that instead of the steady voltage values, an integral term has been used in both voltage sum and difference expressions.

Figure 12 shows the performance of the realized control. One can see that the accuracy of the control is not as good as in the simulation, and in the unstable domain some disturbances occur (time = 80 s). The reason for these effects is first, that the control is not an optimal one, it can be further developed. Second, the implementation of the digital control is still in development stage. There are some communication and implementation issues, which will be handled later, e.g. the integral term is reset at every update of the desired values, so there is a jump in the signal of the phase angle at every new demand. However, the measurements show clearly, that the control is possible in stable and unstable domains as well, even with only two sampled signals per turn.
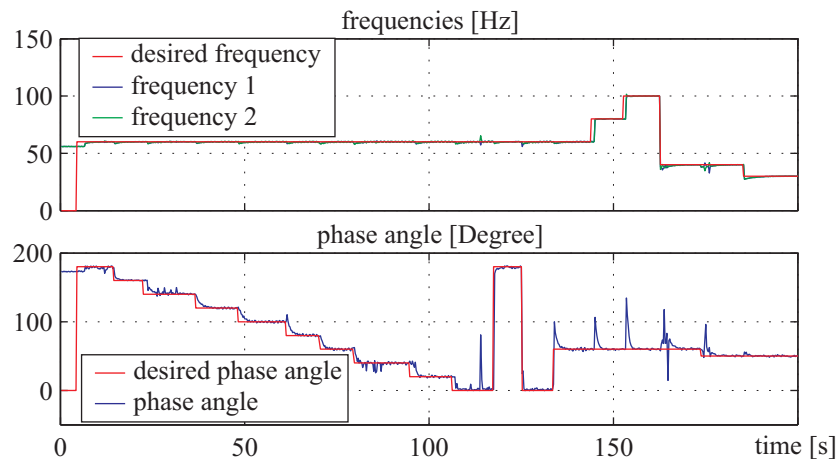

Figure 12: Performance of the Dual Excenter with limited control

5   CONCLUSIONS AND OUTLOOK

In the present work a novel dual-rotor vibrotactor concept has been presented and proved. First, conclusions of analytical investigations have been shown, which allowed us the reliable simulation of the device. Then by means of simulations the phenomenon of mechanical syn-

chronization (and jamming) has been investigated, as well as the possibility of applying a simple controller. The results were encouraging, so a prototype device has been built, on which measurements were carried out. The most important conclusion of the work is that the Dual Excenter concept is feasible, however it still needs further development.

The performance of the realized device can be increased by optimization of the control algorithm. If this does not lead to success, the design of the device can be improved by more accurate signal feedback on frequency and phase angle of the two eccentric rotors.

For building a second and improved prototype device, the simulation parameters could be identified by measurements, and nonlinear and non-isotropic suspension could be considered.

Although measurements show a very good qualitative match to simulations, the mechanical model used for the Dual Excenter has some limitations, as pointed out in Section 2. The most important and critical limitation is, that the motion has been considered as planar motion. As it can be seen on Figure 7, the CoMs of the two rotors of the realized prototype device are not lying in the same plane, normal to the common rotational axis. The consequence of this design is that the generated forces are not in-plane, and so we have excitation also around axes normal to the common rotational axis. This effect could be taken into account with an improved mechanical model.

Finally, for application of the Dual Excenter in tiny handheld devices or in table-top experiments, the overall size of the device should be reduced. Thus, with a well designed controller the Dual Excenter could be an optimal choice for generating vibrations for purposes with high standards.

REFERENCES

[1] J. Brisben, S. S. Hsiao, and K. O. Johnson, Detection of vibration transmitted through an object grasped in the hand. *J Neurophysiol*, **81**, 1548–1558, 1999.

[2] D. A. Mahns, N. M. Perkins, V. Sahai, L. Robinson, and M. J. Rowe, Vibrotactile Frequency Discrimination in Human Hairy Skin. *J Neurophysiol*, **95**, 1442-1450, 2006.

[3] Á. Miklós, Z. Szabó, Vibrator with DC motor driven eccentric rotors. *Periodica Polytechnica - Mechanical Engineering*, **56/1**, 49-53, 2012.

[4] Huygens C, *Horoloqium Oscilatorium*. Paris, 1673.

[5] G. A. Leonov, Phase Synchronization: Theory and Applications. *Automation and Remote Control*, **67/10**, 1573-1609, 2006.

[6] N. V. Kuznetsov, G. A. Leonov, H. Nijmeijer, and A. Pogromsky, Synchronization of two metronomes. *IFAC Proceedings Volumes (IFAC-PapersOnline)*, **3/1**, 49-52, 2007.

[7] K. Czolczynski, P. Perlikowski, A. Stefanski and T. Kapitaniak, Synchronization of pendula rotating in different directions. *Communications in Nonlinear Science and Numerical Simulation*, **17(9)**, 3658–3672, 2012.

[8] X. Liu, C. Wang; C. Zhao; B. Wen, Observation and Control of Phase Difference for a Vibratory Machine of Plane Motion, *2010 International Conference on Computer, Mechatronics, Control and Electronic Engineering (CMCE)*, **4**, 330-334, 2010.